Eur. J. Mineral., 36, 529–540, 2024
https://doi.org/10.5194/ejm-36-529-2024

European Journal of Mineralogy
Open Access

Zvěstovite-(Fe), $Ag_6(Ag_4Fe_2)As_4S_{13}$, a new member of the tetrahedrite group from the Ulatayskoe Ag–Cu–Co occurrence, eastern Siberia, Russia

Cristian Biagioni[1], Anatoly V. Kasatkin[2], Fabrizio Nestola[3], Radek Škoda[4], Vladislav V. Gurzhiy[5], Atali A. Agakhanov[1], and Natalia N. Koshlyakova[6]

[1]Dipartimento di Scienze della Terra, Università di Pisa, Via Santa Maria 53, 56126 Pisa, Italy
[2]Fersman Mineralogical Museum, Russian Academy of Sciences, Leninsky Prospekt 18-2, 119071 Moscow, Russia
[3]Dipartimento di Geoscienze, Università di Padova, Via Gradenigo 6, 35131 Padua, Italy
[4]Department of Geological Sciences, Faculty of Science, Masaryk University, Kotlářská 2, 611 37, Brno, Czech Republic
[5]Department of Crystallography, Institute of Earth Sciences, St Petersburg University, University Emb. 7/9, 199034 Saint Petersburg, Russia
[6]Faculty of Geology, Moscow State University, Vorobievy Gory, 119991 Moscow, Russia

Correspondence: Cristian Biagioni (cristian.biagioni@unipi.it)

Received: 26 March 2024 – Revised: 5 May 2024 – Accepted: 7 May 2024 – Published: 26 June 2024

Abstract. The new mineral zvěstovite-(Fe), ideally $Ag_6(Ag_4Fe_2)As_4S_{13}$, has been found in the small abandoned Ulatayskoe Ag–Cu–Co occurrence, Ovyurskiy District, Tuva Republic, eastern Siberia, Russia. It occurs as anhedral grains, up to 1×0.4 mm in size but usually much smaller, closely intergrown with native silver, in Mg-bearing siderite–quartz gangue. Other associated minerals include acanthite, cobaltite, As-rich members of the tetrahedrite group (kenoargentotennantite-(Fe), tennantite-(Zn), zvěstovite-(Zn)), gersdorffite, jalpaite, krutovite, löllingite, pearceite, safflorite, skutterudite, Br-bearing chlorargyrite, malachite, and muscovite. Zvěstovite-(Fe) is iron black and opaque and has a black streak and metallic lustre. It is brittle and has a conchoidal fracture. No cleavage or parting is observed. The Vickers micro-indentation hardness (Vickers hardness number, VHN; 25 g load) is 169 kg mm^{-2} (range of 149–187 kg mm^{-2}, $n = 4$), corresponding to a Mohs hardness of 3–3.5. The calculated density is 4.979 g cm^{-3}. In reflected light, zvěstovite-(Fe) is light grey with a greenish tint and isotropic. Internal reflections are ubiquitous and deep red in colour. The reflectance values for wavelengths recommended by the Commission on Ore Mineralogy of the International Mineralogical Association are (R, %): 32.5 (470 nm), 31.1 (546 nm), 30.1 (589 nm), and 28.8 (650 nm). The chemical composition (wt %, electron microprobe data, mean of eight spot analyses) is as follows: Cu 1.81, Ag 56.02, Fe 4.60, Zn 0.01, As 13.85, Sb 2.63, S 21.50, total 100.42. The empirical formula, calculated on the basis of 16 atoms per formula unit, is $Ag_{9.93}Cu_{0.54}Fe_{1.58}As_{3.54}Sb_{0.41}S_{12.83}$. Zvěstovite-(Fe) is cubic and has a space group of $I\bar{4}3m$, with $a = 10.8601(3)$, $V = 1280.86(11)$ Å^3, and $Z = 2$. The strongest lines of the X-ray powder diffraction pattern (d, Å (I, %) hkl) are 7.68 (11) 110, 3.136 (100) 222, 2.717 (12) 400, 1.984 (8) 521, 1.921 (23) 440, and 1.638 (11) 622. The crystal structure of zvěstovite-(Fe) was refined to $R_1 = 0.0551$ for 400 unique reflections with $F_o > 4\sigma$ (F_o). The possible ordering of the split $M(2)$ sites is discussed. The new mineral is the Fe isotype of zvěstovite-(Zn). Both these minerals form the zvěstovite series within the tetrahedrite group.

1 Introduction

The tetrahedrite group includes cubic sulfosalts with general formula $^{M(2)}A_6^{M(1)}(B_4C_2)^{X(3)}D_4^{S(1)}Y_{12}^{S(2)}Z$, where A is Cu^+, Ag^+, and □ (vacancy); B is Cu^+ and Ag^+; C is Zn^{2+}, Fe^{2+}, Hg^{2+}, Cd^{2+}, Ni^{2+}, Mn^{2+}, Cu^{2+}, Cu^+, In^{3+}, and Fe^{3+}; D is Sb^{3+}, As^{3+}, Bi^{3+}, and Te^{4+}; Y is S^{2-} and Se^{2-}; and Z is S^{2-}, Se^{2-}, and □ (Biagioni et al., 2020a). This group is one of the fastest-growing and currently includes 40 mineral species. This number is constantly increasing due to the regular approval of new group members by the Commission on New Minerals, Nomenclature and Classification (CNMNC) of the International Mineralogical Association (IMA).

Silver-bearing tetrahedrite-group minerals (Table 1) belong to the following distinct series: (i) the freibergite series (A is Ag, B is Cu, D is Sb), (ii) the arsenofreibergite series (A is Ag, B is Cu, D is As), and (iii) the rozhdestvenskayaite series (A is Ag, B is Ag, and D is Sb). In these three groups, species with both 13 and 12 S atoms per formula unit (apfu) are currently known. In addition to these species, Sejkora et al. (2021) described the As isotype of rozhdestvenskayaite-(Zn), namely zvěstovite-(Zn), ideally $Ag_6(Ag_4Zn_2)As_4S_{13}$.

During the examination of specimens from the Ulatayskoe Ag–Cu–Co occurrence, Ulatay River, Tuva Republic, in eastern Siberia (Russia), a tetrahedrite-group mineral corresponding to the Fe isotype of zvěstovite-(Zn) was identified. This phase, with an ideal composition of $Ag_6(Ag_4Fe_2)As_4S_{13}$, was named zvěstovite-(Fe), in agreement with the nomenclature of the tetrahedrite group (Biagioni et al., 2020a).

The new mineral, its name, and its symbol (Zvě-Fe) have been approved by the CNMNC of the IMA (IMA2022–092, Biagioni et al., 2022a). The holotype specimen is deposited in the systematic collection of the Fersman Mineralogical Museum of the Russian Academy of Sciences, Moscow, with the catalogue number 98050.

In this paper the type description of zvěstovite-(Fe) is reported, and, in agreement with Mills et al. (2009), the zvěstovite series is established.

2 Occurrence and general appearance

Zvěstovite-(Fe) has been found at the Ulatayskoe Ag–Cu–Co occurrence, Ulatay River, Ovyurskiy District, Tuva Republic, eastern Siberia, Russia (50°54′10″ N, 92°16′7″ E).

Geologically, the Ulatayskoe Ag–Cu–Co occurrence belongs to the Ulatay ore field of carbonatites, located on an area of about 20 km^2 in the interfluve of the Ulatay and Teeli rivers. Structurally, all carbonatite outcrops are confined to a large wedge-shaped tectonic ledge controlled by a series of sublatitudinal and northwestern faults. In its central part, schistose volcanogenic–terrigenous deposits of the Lower Devonian, and metamorphic rocks represented by quartz–sericite, mica, and amphibole schists are exposed. Intrusive rocks within the Ulatay ore field are represented by gabbroids of the Torgalyk complex (D_3–C_1). In the north, there is a chain of outcrops of leucocratic biotite granites, linking into a sublatitudinal dike body that cuts gabbroid rocks. Outcrops of late Mesozoic biotite granosyenites are also found within the ore field (Nikiforov et al., 2005).

Ankerite–calcite carbonatites are distributed over the entire area of the Ulatay ore field, while siderite carbonatites are concentrated only in its southern portion. Ore-bearing siderite carbonatites form a dike-like body elongated in the northeastern direction, 150 × 1400 m in size. The hydrothermal Ag–Cu–Co-bearing mineralization is superimposed on the carbonatites. It is represented by veinlets and veins up to 20 cm thick of quartz–sericite–ankerite–calcite–siderite composition, containing silver, skutterudite, safflorite, tetrahedrite-group members (including the new mineral described here), pyrite, chalcopyrite, bornite, and uranium minerals. The veinlets are characterized by a symmetrically zoned structure, and they form stockwork zones often associated with gabbroid bodies. These veinlets are intersected by carbonatite veins, and many probably manifest of an earlier hydrothermal mineralization of the arsenide–cobalt type (Lebedev, 1998; Nikiforov et al., 2005; Prokopyev, 2014).

Zvěstovite-(Fe) occurs as anhedral grains up to 1 × 0.4 mm in size but usually much smaller, closely intergrown with native silver, in Mg-bearing siderite–quartz gangue (Fig. 1). Other associated minerals include acanthite, cobaltite, As-rich members of the tetrahedrite group (kenoargentotennantite-(Fe), tennantite-(Zn), zvěstovite-(Zn)), gersdorffite, jalpaite, krutovite, löllingite, pearceite, safflorite, skutterudite, Br-bearing chlorargyrite, malachite, and muscovite. Zvěstovite-(Fe) can be interpreted as primary and formed by the circulation of low-temperature hydrothermal fluids.

3 Physical properties and optical data

Zvěstovite-(Fe) is iron black and opaque and has a black streak and metallic lustre. It is brittle and has a conchoidal fracture. No cleavage and parting is observed. The Vickers micro-indentation hardness (Vickers hardness number, VHN; 25 g load) is 169 kg mm^{-2} (range of 149–187, $n = 4$), corresponding to a Mohs hardness of 3–3.5. Density could not be measured due to the absence of necessary heavy liquids. Density values calculated using the empirical formulae based on $\Sigma Me = 16$ apfu and $(As + Sb) = 4$ apfu and single-crystal unit-cell parameters are 4.979 and 5.043 g cm^{-3}, respectively.

In reflected light, zvěstovite-(Fe) is light grey with a greenish tint. It is isotropic. Internal reflections are ubiquitous and deep red in colour. Reflectance values have been measured in air using an MSF-R (LOMO, Saint Petersburg, Russia) microspectrophotometer. Silicon was used as a standard. The reflectance values (R) are given in Table 2

Table 1. Members of the tetrahedrite group, where A is Ag.

Species	Chemical formula	a (Å)	V (Å^3)	Ref.
Freibergite series A: Ag, B: Cu, D: Sb				
Argentotetrahedrite-(Cd)	$Ag_6(Cu_4Cd_2)Sb_4S_{13}$	10.65	1208	[1]
Argentotetrahedrite-(Fe)	$Ag_6(Cu_4Fe_2)Sb_4S_{13}$	10.61	1195	[2]
Argentotetrahedrite-(Hg)	$Ag_6(Cu_4Hg_2)Sb_4S_{13}$	10.65	1208	[3]
Argentotetrahedrite-(Zn)	$Ag_6(Cu_4Zn_2)Sb_4S_{13}$	10.57	1180	[4]*
Kenoargentotetrahedrite-(Fe)	$Ag_6(Cu_4Fe_2)Sb_4S_{12}$	10.49	1155	[2]
Kenoargentotetrahedrite-(Zn)	$Ag_6(Cu_4Zn_2)Sb_4S_{12}$	10.46	1145	[5]
Arsenofreibergite series A: Ag, B: Cu, D: As				
Argentotennantite-(Zn)	$Ag_6(Cu_4Zn_2)As_4S_{13}$	10.58	1186	[6]
Kenoargentotennantite-(Fe)	$Ag_6(Cu_4Fe_2)As_4S_{12}$	10.37	1116	[7]
Rozhdestvenskayaite series A: Ag, B: Ag, D: Sb				
Kenorozhdestvenskayaite-(Fe)	$Ag_6(Ag_4Fe_2)Sb_4S_{12}$	10.71	1229	[8]
Rozhdestvenskayaite-(Zn)	$Ag_6(Ag_4Zn_2)Sb_4S_{13}$	10.98	1325	[2]
Zvěstovite series A: Ag, B: Ag, D: As				
Zvěstovite-(Fe)	$Ag_6(Ag_4Fe_2)As_4S_{13}$	10.86	1281	[9]
Zvěstovite-(Zn)	$Ag_6(Ag_4Fe_2)As_4S_{13}$	10.85	1277	[10]

[1] Mikuš et al. (2023). [2] Welch et al. (2018). [3] Wu et al. (2022). [4] Sejkora et al. (2022). [5] Qu et al. (2024a). [6] Spiridonov et al. (1986). [7] Biagioni et al. (2020b). [8] Qu et al. (2024b). [9] This paper. [10] Sejkora et al. (2021). * Sample from Zvěstov, Czech Republic.

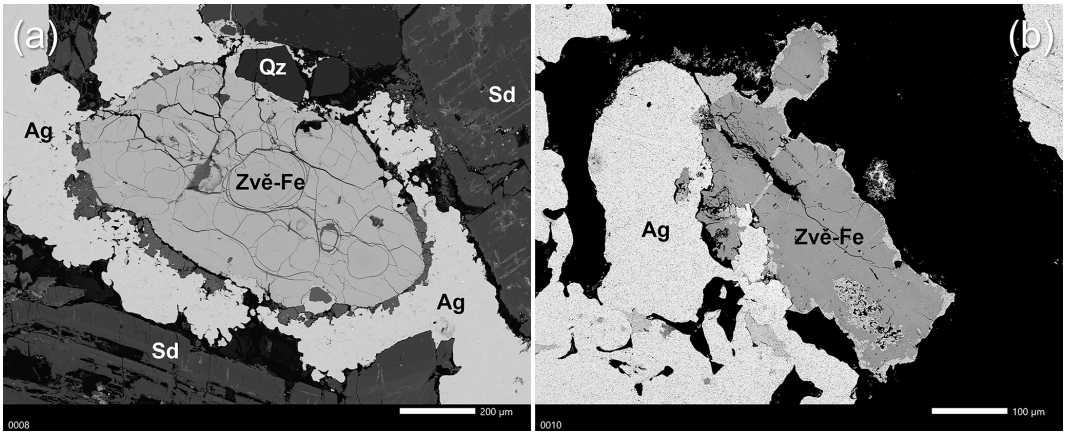

Figure 1. BSE (backscattered electron) image of zvěstovite-(Fe) (Zvě-Fe) grains associated with silver (Ag), siderite (Sd), and quartz (Qz) (mineral symbols after Warr, 2021). The grain shown in **(a)** is the biggest found so far. A part of it was extracted and used for the collection of structural data.

and plotted in Fig. 2 in comparison with the published data for rozhdestvenskayaite-(Zn) (Welch et al., 2018) and zvěstovite-(Zn) (Sejkora et al., 2021).

4 Chemical data

Quantitative chemical analyses were carried out using a Cameca SX100 electron microprobe (WDS mode, wavelength dispersive spectroscopy; 25 kV; 4 nA; 3 µm beam diameter) at the Department of Geological Sciences, Faculty of Science, Masaryk University, Brno, Czech Republic. The re-

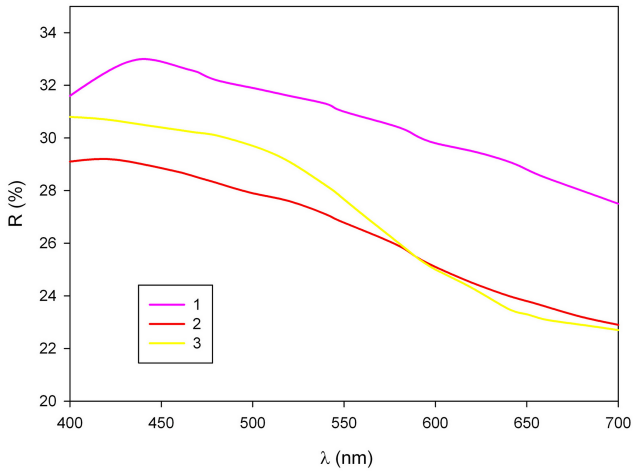

Figure 2. Reflectance curves in air of (1) zvěstovite-(Fe), (2) zvěstovite-(Zn) (Sejkora et al., 2021), and (3) rozhdestvenskayaite-(Zn) (Welch et al., 2018).

Table 2. Reflectance values (in %) for zvěstovite-(Fe).

λ (nm)	*R*	λ (nm)	*R*
400	31.6	560	30.8
420	32.5	580	30.4
440	33.0	**589**	**30.1**
460	32.7	600	29.8
470	**32.5**	620	29.5
480	32.2	640	29.1
500	31.9	**650**	**28.8**
520	31.6	660	28.5
540	31.3	680	28.0
546	**31.1**	700	27.5

Note that the four COM values are shown in bold.

sults (average of five spot analyses) and calibration standards used for quantification are given in Table 3. Contents of other sought elements with atomic numbers $Z > 8$ (including Mn, Co, Ni, Se, Te, Hg, and Bi) are below detection limits. Matrix correction by the PAP algorithm (Pouchou and Pichoir, 1985) was applied to the data.

There are two different approaches to recalculate the chemical formula of the studied samples:

1. normalization on the basis of $\Sigma Me = 16$ apfu, assuming that no vacancies occur at the $M(2)$, $M(1)$, and $X(3)$ sites;

2. normalization on the basis of $(As + Sb) = 4$ apfu, taking into account that previous studies (e.g. Johnson et al., 1986) revealed that negligible variations with respect to the ideal number of atoms hosted at the $X(3)$ site occur.

The first approach gives the formula $Ag_{9.93}Cu_{0.54}Fe_{1.58}As_{3.54}Sb_{0.41}S_{12.83}$, whereas

Table 3. Chemical data (in wt %) for zvěstovite-(Fe).

Element	wt %	Range	SD	Standard
Cu	1.81	1.28–2.88	0.64	Chalcopyrite
Ag	56.02	54.44–57.44	1.07	Ag
Fe	4.60	4.46–4.73	0.10	Chalcopyrite
Zn	0.01	0.00–0.03	0.01	ZnS
As	13.85	13.60–14.04	0.17	Pararammelsbergite
Sb	2.63	2.52–2.82	0.13	Sb
S	21.50	21.26–21.65	0.14	Chalcopyrite
Total	100.42			

the second one corresponds to the formula $Ag_{10.06}Cu_{0.55}Fe_{1.60}(As_{3.58}Sb_{0.42})_{\Sigma 4.00}S_{12.99}$. Taking into account the results of the crystal structure study (see below), these formulae can be rewritten as $Ag_{6.05}(Ag_{3.88}Cu_{0.54}Fe_{1.58})_{\Sigma 6.00}(As_{3.54}Sb_{0.41})_{\Sigma 3.95}S_{12.83}$ and $Ag_{6.21}(Ag_{3.85}Cu_{0.55}Fe_{1.60})_{\Sigma 6.00}(As_{3.58}Sb_{0.42})_{\Sigma 4.00}S_{12.99}$.

The end-member formula of zvěstovite-(Fe) is $Ag_6(Ag_4Fe_2)As_4S_{13}$, corresponding to the following (in wt %): Ag 56.56, Fe 5.86, As 15.72, S 21.86, total 100.00.

5 X-ray crystallography

Powder micro X-ray diffraction (PXRD) data for zvěstovite-(Fe) were collected from the single crystal used for the single-crystal X-ray diffraction (SCXRD) data collection. PXRD data were collected using a Rigaku R-AXIS RAPID II single-crystal diffractometer equipped with a cylindrical image plate detector (radius of 127.4 mm) using Debye–Scherrer geometry, with Co$K\alpha$ radiation (rotating anode with VariMax microfocus optics), at 40 kV and 15 mA. Exposure time was set to 10 min. Angular resolution of the detector is 0.045°2θ (pixel size of 0.1 mm). The data were integrated using the software package `Osc2Tab` (Britvin et al., 2017). Powder X-ray diffraction data of zvěstovite-(Fe) are given in Table 4 in comparison to that calculated from SCXRD data using the `PowderCell` 2.3 software (Kraus and Nolze, 1996). Unit-cell parameters were refined from the observed d spacings using the `UnitCell` software (Holland and Redfern, 1997) and are as follows: $a = 10.863(2)$ Å and $V = 1281.9(8)$ Å^3.

Single-crystal X-ray diffraction intensity data were collected on a grain $0.05 \times 0.04 \times 0.03$ mm^3 in size, extracted from the polished section analysed by electron microprobe (Fig. 1a), using a SuperNova Rigaku Oxford Diffraction single-crystal diffractometer (Mo$K\alpha$ radiation, 50 kV and 0.12 mA working conditions) equipped with a PILATUS 200K DECTRIS detector. The detector-to-crystal distance was 68 mm. Data were collected by 761 frames over 22 runs, in 1° slices, with an exposure time of 60 s per frame and a total time of 12 h. The data were corrected for Lorentz and polarization factors and absorption using the software pack-

Table 4. Powder X-ray diffraction data for zvěstovite-(Fe). I_{calc} and d_{hkl} were calculated using the PowderCell 2.3 software (Kraus and Nolze, 1996) on the basis of the structural model given in Table 6. Only reflections with $I_{calc} > 1$ are listed (if not observed). The strongest reflections are given in bold.

I_{obs}	d_{obs}	$h\ k\ l$	I_{calc}	d_{calc}
11	**7.7**	1 1 0	6	7.679
4	4.43	2 1 1	4	4.434
3	3.440	3 1 0	1	3.434
100	**3.136**	**2 2 2**	**100**	**3.135**
2	2.895	3 2 1	1	2.902
12	**2.717**	**4 0 0**	**19**	**2.715**
2	2.564	3 3 0	4	2.560
–	–	3 3 2	1	2.316
2	2.215	4 2 2	1	2.217
3	2.129	4 3 1	3	2.130
8	**1.984**	**5 2 1**	**11**	**1.983**
23	**1.921**	**4 4 0**	**31**	**1.920**
2	1.863	4 3 3	3	1.862
1	1.814	4 4 2	1	1.810
2	1.764	6 1 1	2	1.762
1	1.763	5 3 2	1	1.762
1	1.720	6 2 0	1	1.717
11	**1.638**	**6 2 2**	**15**	**1.637**
–	–	6 3 1	1	1.601
2	1.568	4 4 4	3	1.568
2	1.536	7 1 0	2	1.534

Table 5. Crystal and experimental data for zvěstovite-(Fe).

Crystal data	
Crystal size (mm)	0.050 × 0.040 × 0.030
Cell setting, space group	Cubic, $I\bar{4}3m$
a (Å)	10.8601(3)
V (Å^3)	1280.86(11)
Z	2
Data collection and refinement	
Radiation, wavelength (Å)	Mo$K\alpha$, $\lambda = 0.71073$
Temperature (K)	293(2)
$2\theta_{max}$ (°)	63.42
Measured reflections	19315
Unique reflections	438
Reflections with $F_o > 4\sigma\ (F_o)$	400
R_{int}	0.1026
$R\sigma$	0.0228
Range of h, k, l	$-16 \le h \le 15$, $-16 \le k \le 16$, $-16 \le l \le 16$
$R\ (F_o > 4\sigma\ (F_o))$	0.0551
R (all data)	0.0618
wR (on F_o)[a]	0.1616
Goof	1.160
Absolute structure[b]	0.00(11)
Number of least-squares parameters	22
Maximum and minimum residual peak (e Å^{-3})	1.70 (at 0.61 Å from M(2b)) −0.96 (at 0.46 Å from M(2b))

[a] $w = 1/[\sigma^2(F_o^2) + (0.0776P)^2 + 18.2805P]$. [b] Flack (1983).

age CrysAlisPro (version 41.64.113a). Zvěstovite-(Fe) is cubic and has a space group of $I\bar{4}3m$, with $a = 10.8601(3)$ Å, $V = 1280.86(11)$ Å^3, and $Z = 2$.

The crystal structure of zvěstovite-(Fe) was refined using SHELXL-2018 (Sheldrick, 2015) starting from the atomic coordinates of zvěstovite-(Zn) (Sejkora et al., 2021), omitting the M(2b) position and modelling the electron density associated with the M(2) site with an unsplit model. The occurrence of a racemic twin was also taken into account. The following neutral scattering curves, taken from the *International Tables for Crystallography* (Wilson, 1992) were used: Ag vs. vacancy at M(2), Ag vs. Fe at M(1), As vs. Sb at X(3), and S at S(1) and S(2) sites. An isotropic model converged to $R_1 = 0.189$, showing a high residual close to the M(2) site, suggesting the split nature of this position. Adding this sub-position, the R_1 factor was lowered to 0.093, indicating the correctness of the structural model. However, correlation values that are too high (> 0.8) were found for the s.o.f. (site occupancy factor) values. Consequently, the s.o.f. values at M(1) and X(3) were fixed on the basis of electron microprobe data, i.e. $^{M(1)}(Ag_{0.64}Fe_{0.27}Cu_{0.09})$ and $^{X(3)}(As_{0.895}Sb_{0.105})$, respectively, whereas the s.o.f. values at M(2a) and M(2b) were freely refined. An anisotropic model for cations was refined to $R_1 = 0.061$. The site occupancy at $M(2a) + M(2b)$ is $Ag_{0.511(8)} + 2 \times Ag_{0.246(5)} = Ag_{1.003}$. For this reason, the s.o.f. at $M(2a) + M(2b)$ was constrained to be 1. An anisotropic model converged to $R_1 = 0.058$. At this stage of refinement, the s.o.f. at the M(1) site was again refined using the Ag vs. Fe scattering curves, improving the refinement. Releasing the constraints on the s.o.f. at X(3), the refinement got worse, and consequently such constraints were not removed. The anisotropic structural model converged to $R_1 = 0.0551$ for 400 reflections with $F_o > 4\sigma\ (F_o)$ and 22 refined parameters. Details of data collection and refinement are given in Table 5. Fractional atomic coordinates and equivalent isotropic displacement parameters are reported in Table 6. Table 7 reports selected bond distances. Bond-valence sums (BVSs) are shown in Table 8. A Crystallographic Information File (CIF) is deposited in the Supplement.

6 Crystal structure description

6.1 General features

The crystal structure of zvěstovite-(Fe) is isotypic with those of other members of the tetrahedrite group (Biagioni et al., 2020a). Indeed, it shows a three-dimensional framework of corner-sharing M(1)-centred tetrahedra delimiting cages hosting S(2)-centred $M(2)_6$ octahedra, surrounded by four $X(3)S(1)_3$ trigonal pyramids. In zvěstovite-(Fe), the M(2) site is split into two sub-positions, as previously reported in

Table 6. Atoms, Wyckoff positions, site occupancy factors (s.o.f.'s), atom coordinates, and equivalent isotropic displacement parameters (Å^2) for zvěstovite-(Fe).

Site	Wyckoff position	s.o.f.	x/a	y/b	z/c	U_{eq}
M(2a)	12e	$Ag_{0.511(5)}$	0.2138(4)	0	0	0.0555(10)
M(2b)	24g	$Ag_{0.244(3)}$	0.2160(6)	−0.0734(6)	0.0734(6)	0.0555(10)
M(1)	12d	$Ag_{0.73(2)}Fe_{0.27(2)}$	1/4	1/2	0	0.0470(3)
X(3)	8c	$As_{0.895}Sb_{0.105}$	0.2537(2)	0.2537(2)	0.2537(2)	0.0346(7)
S(1)	24g	$S_{1.00}$	0.1233(3)	0.1233(3)	0.3518(4)	0.0397(11)
S(2)	2a	$S_{1.00}$	0	0	0	0.050(3)

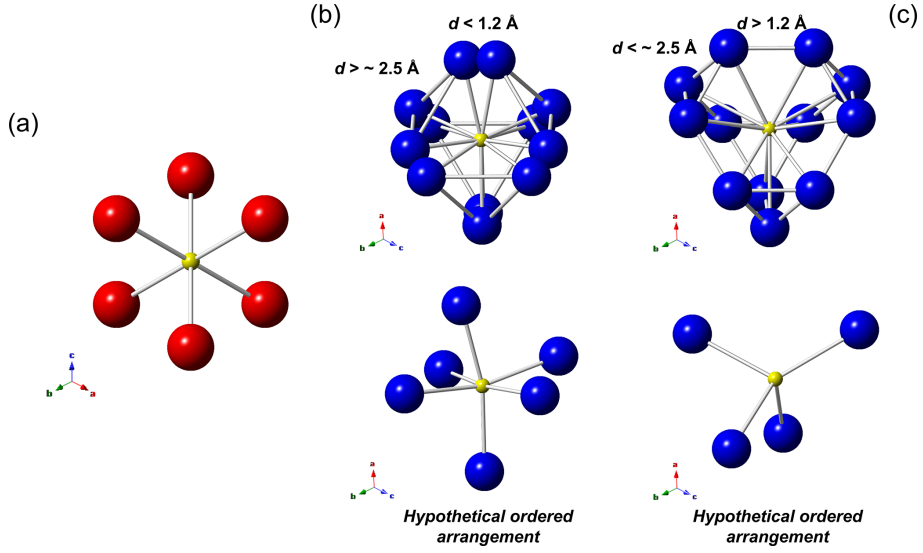

Figure 3. Local arrangements of the M(2a) **(a)** and M(2b) **(b, c)** sites in tetrahedrite-group minerals. In **(b)** and **(c)** two different situations, related to the distances of M(2b)–M(2b), are shown, along with two possible hypothetical ordered atom distributions. M(2a): red circles, M(2b): blue circles, S(2): yellow circles.

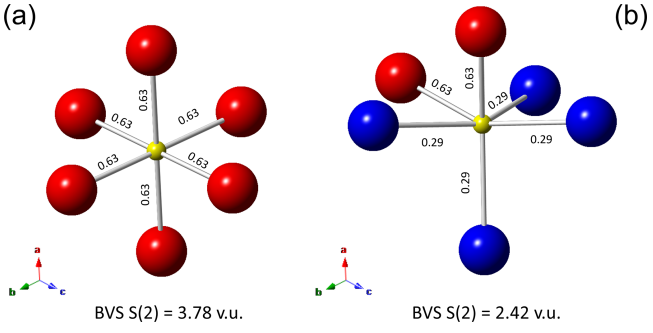

Figure 4. Local arrangements of atoms at the M(2) sites around the S(2) site in zvěstovite-(Fe). In **(a)**, only the M(2a) site is occupied, resulting in a strong overbonding of the S atom at S(2). In **(b)**, a hypothetical ordered distribution of the M(2a) and M(2b) positions, lowering such an overbonding. The values reported along the M(2)–S(2) sites are bond strengths, in valence units (v.u.). Same symbols as in Fig. 3.

Table 7. Selected bond distances (in Å) for zvěstovite-(Fe).

M(1)	– S(1) × 4	2.505(3)
M(2a)	– S(2)	2.322(4)
	– S(1) × 2	2.415(5)
M(2b)	– S(1) × 2	2.603(7)
	– S(2)	2.651(6)
X(3)	– S(1) × 3	2.269(4)

other members of the tetrahedrite group (e.g. Andreasen et al., 2008; Welch et al., 2018).

6.2 Cation sites

In the crystal structure of tetrahedrite isotypes there are three cation sites, namely M(2), M(1), and X(3).

In zvěstovite-(Fe), the electron density associated with the M(2) site is actually split into two sub-sites, M(2a)

Table 8. Weighted bond-valence sums (in valence units) in zvěstovite-(Fe).

Site	$M(1)$	$M(2a)$	$M(2b)$	$X(3)$	Σanions	Theoretical
S(1)	$^{2\times\rightarrow}0.37^{\times4\downarrow}$	$0.25^{\times2\downarrow}$	$^{2\times\rightarrow}0.06^{\times2\downarrow}$	$1.04^{\times3\downarrow}$	2.15	2.00
S(2)		$^{6\times\rightarrow}0.32$	$^{12\times\rightarrow}0.07$		2.76	2.00
Σcations	1.48	0.82	0.19	3.12		
Theoretical	1.33	0.51	0.24	3.00		

Note that bond-valence sums were weighted according to the site occupancies discussed in the text and using the bond parameters of Brese and O'Keeffe (1991).

and $M(2b)$. These two positions cannot be simultaneously populated, owing to the short $M(2a)$–$M(2b)$ distance, i.e. ∼ 1.13 Å. The $M(2b)$–$M(2b)$ distance is 2.19(12) Å. These distances are slightly longer than those reported by Sejkora et al. (2021) for zvěstovite-(Zn), i.e. $M(2a)$–$M(2b) = 1.00(5)$ Å and $M(2b)$–$M(2b) = 1.97(11)$ Å. Moreover, these values can be compared with those of Cu-excess tennantite-(Cu) described by Makovicky et al. (2005), with Cu2A–Cu2B and Cu2B–Cu2B distances of 1.08(2) and 2.00(3) Å, respectively. It is worth noting that, with respect to Cu-excess tennantite, no Ag excess was detected during the crystal structure refinement of zvěstovite-(Fe). The site occupancy at the $M(2a)$ and $M(2b)$ sites was refined to $Ag_{0.51}$ and $Ag_{0.24}$, respectively, corresponding (considering site multiplicity) to a virtual full occupancy of Ag at the $M(2)$ site. The ⟨$M(2a)$–S⟩ and ⟨$M(2b)$–S⟩ average distances are 2.384 and 2.635 Å, respectively. In the Zn isotype zvěstovite-(Zn), such distances are 2.39 and 2.57 Å, respectively. The ⟨$M(2a)$–S⟩ distance is too short for an Ag-bearing site, as proved by the overbonding of atoms hosted at $M(2a)$ (BVS = 1.61 v.u., valence unit, if assumed fully occupied by Ag), similar to that reported by Sejkora et al. (2021) for zvěstovite-(Zn). This short distance can probably be interpreted as being due to the aspherical coordination of 3-fold Ag, as highlighted by Johnson et al. (1988); this behaviour was also discussed by Welch et al. (2018). These authors showed that the $M(2)$–S(1) distance is more sensitive to the Ag content, whereas the increase in the $M(2)$–S(2) distance is usually smaller. On the contrary, the ⟨$M(2b)$–S⟩ distance is slightly larger than the ideal one for 3-fold coordinated Ag atoms, resulting in a slight underbonding (0.81 v.u., assuming the full occupancy by Ag).

The tetrahedrally coordinated $M(1)$ site has a bond distance of 2.505(3) Å, in agreement with the $M(1)$–S(1) distances reported for rozhdestvenskayaite-(Zn), i.e. 2.496(2) Å (Welch et al., 2018), and zvěstovite-(Zn), i.e. 2.497(6) Å (Sejkora et al., 2021). On the basis of electron microprobe data, the site occupancy $(Ag_{0.65}Cu_{0.09}Fe_{0.26})$ can be proposed. This corresponds to a mean atomic number of 39.92 electrons, compared with a refined mean atomic number of 41.33 electrons. The bond-valence sum is 1.48 v.u., in agreement with the theoretical value of 1.33 v.u., calculated assuming Ag and Cu as monovalent cations and Fe as Fe^{2+} and Fe^{3+}, on the basis of the site population $[(Ag^{+}_{3.88}Cu^{+}_{0.12})(Cu^{+}_{0.42}Fe^{3+}_{0.42}Fe^{2+}_{1.16})]$.

The $X(3)$ site has a bond distance of 2.269(4) Å, and it shows a mixed (As, Sb) site occupancy. On the basis of electron microprobe data, the site occupancy was fixed to $(As_{0.895}Sb_{0.105})$, resulting in a BVS of 3.12 v.u.

6.3 Anion sites

Two anion sites, S(1) and S(2), occur in the crystal structure of tetrahedrite-group minerals. Whereas the former is always occupied, S(2) can be at least partially empty, explaining the variability in S content observed in these compounds.

The anion hosted at S(1) is tetrahedrally coordinated by two atoms hosted at $M(1)$, one at $M(2)$ ($M(2a)$ or one of the two mutually exclusive $M(2b)$ sites) and one at $X(3)$. In zvěstovite-(Fe), the S(1) is fully occupied by S atoms, and the bond-valence sum is 2.15 v.u.

A more complex situation can be found around the S(2) site. Indeed, as in zvěstovite-(Zn), the S atom at this position is overbonded, owing to metal–S bonds that are too short. However, as will be discussed below, an ordered distribution of $M(2a)$ and $M(2b)$ positions around S(2) could favour the achievement of a more reasonable bond-valence sum.

The S(1) and S(2) sites were found fully occupied. The volume of the S(2)$[M(2)]_6$ octahedron, calculated using the $M(2a)$ position, is ∼ 16.8 Å^3, comparable with the volume observed in rozhdestvenskayaite-(Zn), i.e. 15.9 Å^3 (Welch et al., 2018), and slightly larger than the value observed by Sejkora et al. (2021), i.e. 15.4 Å^3, for zvěstovite-(Zn).

7 Discussion

7.1 Ordering of $M(2)$ split sites in tetrahedrite-group minerals

The first descriptions of the splitting of the $M(2)$ site in tetrahedrite-group compounds were reported in the 2000s. Makovicky et al. (2005), using single-crystal X-ray diffraction techniques, found a relatively strong residual at ∼ 1 Å from the $M(2)$ site in a sample of tennantite-(Cu) from Cerro Atajo, Argentina, first proposing a splitting of this site into two partially occupied positions. Later, Andreasen et al. (2008), on the basis of Rietveld refinement of neu-

tron powder diffraction data, observed the same feature on synthetic members of the series $Cu_{12-x}Fe_xSb_4S_{13}$. It is worth noting that the first hypothesis about the possible splitting of this site was put forward at the end of the 1970s by Makovicky and Skinner (1979), who noted the marked anisotropic displacement parameter of $M(2)$ perpendicular to the $M(2)S_3$ triangle plane. Welch et al. (2018) reported the splitting of the $M(2)$ site in rozhdestvenskayaite-(Zn), thus suggesting that site splitting may also affect Ag-hosting positions. Since the approval of the nomenclature of tetrahedrite-group minerals, several crystal-chemical investigations on different members of this isotypic group have been performed. In several cases, split $M(2)$ sites were modelled. Table 9 summarizes some crystal-chemical features of the $M(2a)$ and $M(2b)$ sites, i.e. the $Ag/(Cu + Ag)$ atomic ratios, as obtained from electron microprobe analyses, the refined site occupancies at the two split positions, and cation–cation and cation–anion distances.

In a static model, the $M(2a)$ site octahedrally coordinates the S atom hosted at S(2) (Fig. 3a). The variation in $M(2a)$–S(2) distance with the increasing $Ag/(Cu + Ag)$ atomic ratio is smaller than expected (considering the different size of Cu and Ag), ranging between 2.21 and 2.32 Å, resulting in the overbonding of S atoms in Ag-rich samples. $M(2a)$ and $M(2b)$ are mutually exclusive since their $M(2a)$–$M(2b)$ distance is always shorter than 1.15 Å, with the longer ones being observed in zvěstovite-(Fe) and tennantite-(Ni), i.e. 1.13 Å. Considering the second coordination sphere, $M(2a)$ shows physically reasonable distances with $M(2b)$, in the range of 2.72–3.05 Å, and with $M(2a)$, in the interval between 3.12 and 3.28 Å. In this latter case, such distances indicate that no cation–cation interaction probably takes place, whereas some $M(2a)$–$M(2b)$ distances, e.g. 2.91 Å in zvěstovite-(Fe), may be comparable to Ag–Ag distances in metallic Ag, i.e. 2.89 Å (Suh et al., 1988), thus possibly suggesting some kind of metallic interaction.

When $M(2b)$ is occupied, 12 cation positions are located around S(2), forming a truncated tetrahedron, known as a Laves polyhedron. The $M(2b)$–S(2) distances are more variable than the $M(2a)$–S(2) ones. In particular, they are significantly elongated when $M(2)$ is fully occupied by Ag, i.e. 2.56–2.61 Å. It is also worth noting that in this argentiferous species the site occupancy at $M(2b)$ is higher than in Ag-poorer or Ag-free species, indicating a tendency for Ag to occupy this position. The 12 positions around S(2) cannot be occupied simultaneously, as indicated by the $M(2b)$–$M(2b)$ distances that are too short, i.e. $d < 2.25$ Å. Two distinct groups of distances can be identified, i.e. shorter and longer than ∼ 1.2 Å. This threshold has an implication. Indeed, if the distance of the $M(2b)$ positions is shorter than ∼ 1.2 Å, then the three $M(2b)$ positions forming the triangular faces of the Laves polyhedron can form physically reasonable distances (Fig. 3b). On the contrary, contacts that are too short and unrealistic among these three $M(2b)$ atoms occur (Fig. 3c). To establish if a distance is physically meaningful

Table 9. Geometrical features of $M(2)$ sites in tetrahedrite-group minerals. Distances are given in ångströms (Å).

Species	$Ag/(Cu + Ag)_{at.}$	$M(2a)$	$M(2b)$	$M(2a)$				$M(2b)$			U_{eq}	Ref.
		s.o.f.	s.o.f.	S(2)	$M(2b)$	$M(2b)$	X(3)	S(2)	$M(2b)$	$M(2b)$	X(3)	(Å^2)	
Stibiogoldfieldite	0.00[a]	$Cu_{0.73}$	$Cu_{0.08}$	2.21	0.52	2.92	3.12	3.48	2.30	1.04	2.64	2.96	0.032	[1]
Tennantite-(Cd)	0.00	$Cu_{0.84}$	$Cu_{0.08}$	2.21	0.84	2.81	3.13	3.54	2.38	1.68	2.30	2.70	0.038	[2]
Tennantite-(Cu)	0.00[b]	$Cu_{0.75}$	$Cu_{0.17}$	2.21	1.08	2.72	3.13	3.48	2.43	2.16	2.00	2.41	0.046/0.050	[3]
Tennantite-(Cu)	0.00	$Cu_{0.67}$	$Cu_{0.165}$	2.21	0.60	2.88	3.12	3.43	2.30	1.20	2.54	2.84	0.034	[4]
Tennantite-(Ni)	0.00	$Cu_{0.69}$	$Cu_{0.155}$	2.25	1.13	2.72	3.18	3.48	2.42	2.24	1.93	2.37	0.041	[5]
Stibioústalečite	0.02[c]	$Cu_{0.83}$	$Cu_{0.08}$	2.23	0.75	2.86	3.15	3.59	2.37	1.51	2.43	2.84	0.048	[6]
Arsenoústalečite	0.03	$Cu_{0.76}$	$Cu_{0.12}$	2.23	1.00	2.81	3.15	3.60	2.46	1.99	2.18	2.60	0.051	[6]
Tetrahedrite-(Cd)	0.06	$Cu_{0.63}$	$Cu_{0.19}$	2.24	0.43	3.01	3.17	3.49	2.32	0.85	2.80	3.07	0.036	[7]
Tennantite-(Hg)	0.18[c]	$Cu_{0.81}$	$Ag_{0.095}$	2.31	0.88	2.82	3.26	3.57	2.33	1.74	2.19	2.72	0.040	[8]
Argentotetrahedrite-(Zn)	0.53	$Ag_{0.54}$	$Cu_{0.23}$	2.29	0.54	2.94	3.24	3.47	2.26	1.06	2.58	2.95	0.042	[9]
Argentotetrahedrite-(Zn)	0.54	$Ag_{0.52}$	$Cu_{0.24}$	2.30	0.45	3.01	3.25	3.46	2.28	0.89	2.72	3.02	0.039	[9]
Argentotetrahedrite-(Zn)	0.54	$Ag_{0.67}$	$Cu_{0.165}$	2.26	0.36	3.03	3.19	3.46	2.28	0.70	2.83	3.11	0.055	[9]
Rozhdestvenskayaite-(Zn)	1.00	$Ag_{0.53}$	$Ag_{0.24}$	2.28	0.79	3.05	3.23	3.71	2.56	1.54	2.69	2.93	0.050/0.049	[10]
Zvěstovite-(Fe)	1.00	$Ag_{0.51}$	$Ag_{0.24}$	2.32	1.13	2.91	3.28	3.80	2.60	2.19	2.25	2.68	0.056	[11]
Zvěstovite-(Zn)	1.00[b]	$Ag_{0.53}$	$Ag_{0.24}$	2.26	1.00	2.96	3.19	3.71	2.61	1.97	2.44	2.72	0.048/0.052	[12]

[1] Museti et al. (2024). [2] Biagioni et al. (2022b). [3] Makovicky et al. (2005). [4] Biagioni et al. (2022c). [5] Wang et al. (2023). [6] Sejkora et al. (2024). [7] Sejkora et al. (2023). [8] Biagioni et al. (2021). [9] Sejkora et al. (2022). [10] Welch et al. (2018). [11] This paper. [12] Sejkora et al. (2021). [a] Vacancy occurs at the $M(2)$ site (∼ 0.7 apfu). [b] Possible metal excess (up to 0.5 apfu). [c] Possible occurrence of minor vacancy (less than 0.5 apfu).

Table 10. Comparative data for zvěstovite-(Fe) and zvěstovite-(Zn).

Mineral	Zvěstovite-(Fe)	Zvěstovite-(Zn)
End-member formula	$Ag_6(Ag_4Fe_2)As_4S_{13}$	$Ag_6(Ag_4Zn_2)As_4S_{13}$
Crystal-chemical empirical formula ($\Sigma Me = 16$ apfu)	$Ag_{6.00}(Ag_{3.93}Cu_{0.54}Fe_{1.58})(As_{3.54}Sb_{0.41})_{\Sigma 3.95}S_{12.83}$	$Ag_{6.27}(Ag_{3.90}Cu_{0.38}Zn_{1.60}Fe_{0.09}Cd_{0.03})(As_{2.26}Sb_{1.48})_{\Sigma 3.74}S_{12.50}$
Crystal system, space group	Cubic, $I\bar{4}3m$	Cubic, $I\bar{4}3m$
a (Å)	10.8601(3)	10.850(2)
V (Å^3)	1280.86(11)	1277.3(8)
Z	2	2
Colour	Iron black	Grey
Streak	Black	Grey
Lustre	Metallic	Metallic
Transparency	Opaque	Opaque
Tenacity	Brittle	Brittle
Cleavage	Not observed	Not observed
Fracture	Conchoidal	Conchoidal
Calculated density (g cm^{-3})	4.979	5.16
Optical properties (reflected light):		
Colour	Light grey with a greenish tint	Grey with a greenish tint
Bireflectance	Absent	Absent
Pleochroism	Absent	Absent
Anisotropy	Isotropic	Isotropic
Internal reflections	Dark red, ubiquitous	Dark red, ubiquitous
COM reflectance values (R, %):		
470 nm	32.5	28.5
546 nm	31.1	26.9
589 nm	30.1	25.5
650 nm	28.8	23.8
Reference	This paper	Sejkora et al. (2021)

or not one can consider the Ag–Ag and Cu–Cu distances in metallic silver and copper, i.e. 2.89 and 2.55 Å, respectively (Suh et al., 1988). Consequently, $d \sim 2.8$ Å and ~ 2.5 Å can be proposed as cutoff values for Ag- and Cu-bearing phases. Distances longer than these values can be considered physically reasonable, giving rise to hypothetically ordered arrangements resulting in a distorted octahedral coordination around S(2) (Fig. 3b). On the contrary, distances shorter than the cutoff values may indicate that only some positions can be occupied. In particular, only 4 positions out of 12 (i.e. one-third) can be occupied in this latter case (Fig. 3c). The coordination around S(2) can be completed considering an ordered arrangement involving both M(2a) and M(2b) positions (see below).

In zvěstovite-(Fe), the occurrence of Ag atoms at M(2a) results in a strong overbonding of S atoms at S(2) (Fig. 4a). The occupancy of only 4 out of 12 M(2b) positions would give a bond-valence sum of 1.16 v.u. at the S atoms at S(2), i.e. a severe underbonding. Moreover, it would result in an Ag deficit, not observed during electron microprobe analysis. For this reason, a possible ordered arrangement with four M(2b) sites and two M(2a) sites, as shown in Fig. 4b, would help in giving more reasonable bond-valence sums. In particular, such a distribution would result in the site occupancies $M(2a) = Ag_{0.33}$ and $M(2b) = Ag_{0.33}$, i.e. $^{M(2)}[^{M(2a)}Ag_{0.33}^{M(2b)}(Ag_{0.67})]$, considering site multiplicity. These values are different from those observed during crystal structure refinements. Considering only Ag-pure phases, i.e. rozhdestvenskayaite-(Zn), zvěstovite-(Zn), and zvěstovite-(Fe), the following site occupancies at M(2) can be written, respectively: $^{M(2)}[^{M(2a)}Ag_{0.53}^{M(2b)}(Ag_{0.47})]$, $^{M(2)}[^{M(2a)}Ag_{0.53}^{M(2b)}(Ag_{0.47})]$, and $^{M(2)}[^{M(2a)}Ag_{0.51}^{M(2b)}(Ag_{0.49})]$. This seems to indicate a similar preference of Ag for M(2a) and M(2b), different from that observed in Cu phases, where M(2a) is distinctly more populated (Table 9). The discrepancy with the static ordered model could be due to the interplay between static and dynamic disorder. Indeed, it is not clear if what observed

is the average of the ordered distribution of atoms associated with the $M(2)$ site in different cells or if the disorder could be (also) due to the mobility of Cu and Ag atoms. This latter feature is indeed well-known in some Cu and Ag chalcogenides (e.g. Bindi et al., 2020).

7.2 The zvěstovite series

Zvěstovite-(Fe) and zvěstovite-(Zn) form the zvěstovite series within the tetrahedrite group (Biagioni et al., 2020a). These species are the As isotypes of the members of the rozhdestvenskayaite series. Table 10 compares the properties of the two members of the newly established series.

Note that according to our data zvěstovite-(Zn) also occurs in the Ulatayskoe Ag–Cu–Co occurrence and has the composition $Ag_{8.58}Cu_{1.66}Zn_{1.48}Fe_{0.28}As_{3.72}Sb_{0.28}S_{12.89}$. It is probably the third occurrence worldwide of this mineral after its type locality, Zvěstov (Sejkora et al., 2021), and the Frische Lutter vein near Bad Lauterberg in Lower Saxony, Germany (Koch and Heider, 2018). In comparison with zvěstovite-(Fe), zvěstovite-(Zn) from the Ulatayskoe Ag–Cu–Co occurrence is significantly poorer in Ag and richer in Cu. Its structure was not studied, and its identification is based on chemical data only.

Finally, a potential occurrence of zvěstovite-(Fe) was reported by Gan (1980) from the Manson Lode deposit, North Kentalan, Malaysia.

8 Conclusion

In the last decade, the increasing amount of structural data collected on tetrahedrite-group minerals has allowed for addressing some structural issues like, for instance, the role of Ag in these important chalcogenides. In addition to the formation of $[Ag_6]^{4+}$ clusters, coupled with the formation of vacancy at the S(2) site (Welch et al., 2018), new species with up to 10 Ag apfu and no S vacancy have been discovered, being characterized by both Sb^{3+} and As^{3+} as D chemical constituents (Welch et al., 2018; Sejkora et al., 2021). These studies suggested some possible mechanisms favouring the full occupancy of Ag at the $M(2)$ site and S at the S(2) site of the crystal structure of tetrahedrite-group minerals. For instance, Sejkora et al. (2021) hypothesized the possible displacement of S atoms from the special position (0, 0, 0) in order to achieve more reasonable Ag–S distances. In the present study, the possible ordered distribution of Ag between $M(2a)$ and $M(2b)$ positions is also suggested as a further mechanism for lowering the overbonding of S atoms at S(2).

Silver-bearing tetrahedrites, belonging to four different series within the tetrahedrite group, still represent an intriguing crystal-chemical challenge for mineralogists and materials scientists. Their secrets may be revealed only through the examination of more and more samples, possibly examining them not only at room temperature but also at non-ambient conditions, using a multi-technique approach.

Data availability. Crystallographic data for zvěstovite-(Fe) are available in the Supplement.

Supplement. The supplement related to this article is available online at: https://doi.org/10.5194/ejm-36-529-2024-supplement.

Author contributions. CB and AVK conceived the project and wrote the paper with input from other authors. CB and FN performed single-crystal X-ray measurements and interpreted the data. AVK discovered the mineral and performed optical measurements. RŠ, AVK, and NNK performed EMPA (electron microprobe analysis) measurements. VVG provided powder X-ray data collection. AAA performed hardness measurements.

Competing interests. At least one of the (co-)authors is a member of the editorial board of *European Journal of Mineralogy*. The peer-review process was guided by an independent editor, and the authors also have no other competing interests to declare.

Disclaimer. Publisher's note: Copernicus Publications remains neutral with regard to jurisdictional claims made in the text, published maps, institutional affiliations, or any other geographical representation in this paper. While Copernicus Publications makes every effort to include appropriate place names, the final responsibility lies with the authors.

Special issue statement. This article is part of the special issue "New minerals: EJM support". It is not associated with a conference.

Acknowledgements. We appreciate the many constructive comments of Kai Qu and an anonymous reviewer that helped to improve this paper significantly.

Financial support. Publisher's note: the article processing charges for this publication were not paid by a Russian or Belarusian institution.

Review statement. This paper was edited by Sergey Krivovichev and reviewed by Kai Qu and one anonymous referee.

References

Andreasen, J. W., Makovicky, E., Lebech, B., and Karup-Møller, S.: The role of iron in tetrahedrite and tennantite determined by

Rietveld refinement of neutron powder diffraction data, Phys. Chem. Miner., 35, 447–454, 2008.

Biagioni, C., George, L. G., Cook, N. J., Makovicky, E., Moëlo, Y., Pasero, M., Sejkora, J., Stanley, C. J., Welch, M. D., and Bosi, F.: The tetrahedrite group: Nomenclature and classification, Am. Mineral., 105, 109–122, 2020a.

Biagioni, C., Sejkora, J., Moëlo, Y., Makovicky, E., Pasero, M., and Dolníček, Z.: Kenoargentotennantite-(Fe), IMA 2020-062, in: CNMNC Newsletter 58, Eur. J. Mineral., 32, https://doi.org/10.5194/ejm-32-645-2020, 2020b.

Biagioni, C., Sejkora, J., Raber, T., Roth, P., Moëlo, Y., Dolníček, Z., and Pasero, M.: Tennantite-(Hg), $Cu_6(Cu_4Hg_2)As_4S_{13}$, a new tetrahedrite-group mineral from the Lengenbach quarry, Binn, Switzerland, Mineral. Mag., 85, 744–751, 2021.

Biagioni, C., Kasatkin, A. V., Nestola, F., Škoda, R., Agakhanov, A. A., and Koshlyakova, N. N.: Zvěstovite-(Fe), IMA 2022-092, in: CNMNC Newsletter 70, Eur. J. Mineral., 34, https://doi.org/10.5194/ejm-34-591-2022, 2022a.

Biagioni, C., Kasatkin, A. V., Sejkora, J., Nestola, F., and Škoda, R.: Tennantite-(Cd), $Cu_6(Cu_4Cd_2)As_4S_{13}$, from the Berenguela mining district, Bolivia: the first Cd-member of the tetrahedrite group, Mineral. Mag., 86, 834–840, 2022b.

Biagioni, C., Sejkora, J., Moëlo, Y., Marcoux, E., Mauro, D., and Dolníček, Z.: Tennantite-(Cu), $Cu_{12}As_4S_{13}$, from Layo, Arequipa Department, Peru: a new addition to the tetrahedrite-group minerals, Mineral. Mag., 86, 331–339, 2022c.

Bindi, L., Nespolo, M., Krivovichev, S. V., Chapuis, G., and Biagioni, C.: Producing highly complicated materials. Nature does it better, Rep. Prog. Phys. 83, 106501, https://doi.org/10.1088/1361-6633/abaa3a, 2020.

Brese, N. E. and O'Keeffe, M.: Bond-valence parameters for solids, Acta Crystallogr. B, 47, 192–197, 1991.

Britvin, S. N., Dolivo-Dobrovolsky, D. V., and Krzhizhanovskaya, M. G.: Software for processing the X-ray powder diffraction data obtained from the curved image plate detector of Rigaku RAXIS Rapid II diffractometer, Zapiski Rossiiskogo Mineralogicheskogo Obshchestva, 146, 104–107, 2017 (in Russian).

Flack, H. D.: On enantiomorph-polarity estimation, Acta Crystallogr. A, 39, 876–881, 1983.

Gan, L. C.: Manson Lode, a stratabound base metal-silver deposit in North Kelantan, Malaysia, unpublished thesis, Montan-Universität Leoben, Austria, 171 pp., 1980.

Holland, T. J. B. and Redfern, S. A. T.: Unit cell refinement from powder diffraction data: the use of regression diagnostics, Mineral. Mag., 61, 65–77, 1997.

Johnson, N. E., Craig, J. R., and Rimstidt, J. D.: Compositional trends in tetrahedrite, Can. Mineral., 24, 385–397, 1986.

Johnson, N. E., Craig, J. R., and Rimstidt, J. D.: Crystal chemistry of tetrahedrite, Am. Mineral., 73, 389–397, 1988.

Koch, H.-P. and Heider, K.-J.: Die Selenid-Mineralisation der Grube "Frische Lutter" bei Bad Lauterbach, Harz, Der Aufschluss, 69, 1–21, 2018 (in German).

Kraus, W. and Nolze, G.: POWDER CELL – a program for the representation and manipulation of crystal structures and calculation of the resulting X-ray powder patterns, J. Appl. Cryst., 29, 301–303, 1996.

Lebedev, V. I.: Ore-magmatic systems of reference arsenide-cobalt deposits, Novosibirsk, SO RAN, 136 pp., 1998 (in Russian).

Makovicky, E. and Skinner, B. J.: Studies of the sulfosalts of copper. VII. Crystal structures of the exsolution products $Cu_{12.3}Sb_4S_{13}$ and $Cu_{13.8}Sb_4S_{13}$ of unsubstituted synthetic tetrahedrite, Can. Mineral., 17, 619–634, 1979.

Makovicky, E., Karanović, L., Poleti, D., Balić-Zunić, T., and Paar, W. H.: Crystal structure of copper-rich unsubstituted tennantite, $Cu_{12.5}As_4S_{13}$, Can. Mineral., 43, 679–688, 2005.

Mikuš, T., Vlasáč, J., Majzlan, J., Sejkora, J., Steciuk, G., Plášil, J., Rößler, C., and Matthes, C.: Argentotetrahedrite-(Cd), $Ag_6(Cu_4Cd_2)Sb_4S_{13}$, a new member of the tetrahedrite group from Rudno nad Hronom, Slovakia, Mineral. Mag., 87, 262–270, 2023.

Mills, S. J., Hatert, F., Nickel, E. H., and Ferraris, G.: The standardisation of mineral group hierarchies: application to recent nomenclature proposals, Eur. J. Miner., 21, 1073–1080, https://doi.org/10.1127/0935-1221/2009/0021-1994, 2009.

Musetti, S., Sejkora, J., Biagioni, C., and Dolníček, Z.: Tellurium-rich stibiogoldfieldite and Se-bearing dantopaite from Goldfield, Nevada, USA: new crystal chemical data, Mineral. Mag., 88, 40–48, 2024.

Nikiforov, A. V., Bolonin, A. V., Sugorakova, A. M., Popov, V. A., and Lykhin, D. A.: Carbonatites of Central Tuva: geological structure, mineral and chemical composition, Geol. Ore Deposit., 47, 360–382, 2005.

Pouchou, J. L. and Pichoir, F.: "PAP" ($\varphi\rho$Z) procedure for improved quantitative microanalysis, in: Microbeam Analysis, edited by: Armstrong, J. T., 104–106, San Francisco Press, San Francisco, 1985.

Prokopyev, I. R.: Geological and physic-chemical conditions for the formation of Fe-F-REE carbonatites of Central Tuva, PhD Thesis, Novosibirsk, 152 pp., 2014 (in Russian).

Qu, K., Sima, X., Gu, X., Sun, W., Fan, G., Yang, Z., and Wang, Y.: Kenoargentotetrahedrite-(Zn), $[Ag_6]^{4+}(Cu_4Zn_2)Sb_4S_{12}\square$, a new member of the tetrahedrite group from the Yindongpo Au deposit, China, Eur. J. Mineral., 36, 397–409, https://doi.org/10.5194/ejm-36-397-2024, 2024a.

Qu, K., Su, W., Nestola, F., Gu, X., Yang, Z., Sima, X., Tang, C., Fan, G., and Wang, Y.: Kenorozhdestvenskayaite-(Fe), $Ag_6(Ag_4Fe_2)Sb_4S_{12}\square$: A new tetrahedrite-group mineral containing a natural $[Ag_6]^{4+}$ cluster and its relationship to the synthetic ternary phosphide $(Ag_6M_4P_{12})M'_6$, Am. Mineral., https://doi.org/10.2138/am-2023-9074, online first, 2024b.

Sejkora, J., Biagioni, C., Vrtiška, L., and Moëlo, Y.: Zvěstovite-(Zn), $Ag_6(Ag_4Zn_2)As_4S_{13}$, a new tetrahedrite-group mineral from Zvěstov, Czech Republic, Mineral. Mag., 85, 716–724, 2021.

Sejkora, J., Biagioni, C., Števko, M., Raber, T., Roth, P., and Vrtiška, L.: Argentotetrahedrite-(Zn), $Ag_6(Cu_4Zn_2)Sb_4S_{13}$, a new member of the tetrahedrite group, Mineral. Mag., 86, 319–330, 2022.

Sejkora, J., Biagioni, C., Škácha, P., Musetti, S., Kasatkin, A. V., and Nestola, F.: Tetrahedrite-(Cd), $Cu_6(Cu_4Cd_2)Sb_4S_{13}$, from Radětice near Příbram, Czech Republic: the new Cd member of the tetrahedrite group, Eur. J. Mineral., 35, 897–907, https://doi.org/10.5194/ejm-35-897-2023, 2023.

Sejkora, J., Biagioni, C., Škácha, P., Musetti, S., and Mauro, D.: Arsenoústalečite, $Cu_{12}(As_2Te_2)Se_{13}$, a new mineral, and crystal structures of arsenoústalečite and stibioústalečite, Mineral. Mag., 88, 127–135, https://doi.org/10.1180/mgm.2023.94, 2024.

Sheldrick, G. M.: Crystal structure refinement with SHELXL, Acta Crystallogr. C, 71, 3–8, 2015.

Spiridonov, E. M., Sokolova, N. G., Gapeev, A. K., Dashevskaya, D. M., Evstigneeva, T. L., Chvileva, T. N., Demidov, V. G., Balashov, E. P., and Shulga, V. I.: A new mineral – argentotennantite, Dokl. Akad. Nauk SSSR, 290, 206–210, 1986 (in Russian).

Suh, I. K., Ohta, H., and Waseda, Y.: High-temperature thermal expansion of six metallic elements measured by dilatation method and X-ray diffraction, J. Mater. Sci., 23, 757–760, 1988.

Wang, Y., Chen, R., Gu, X., Hou, Z., Nestola, F., Yang, Z., Fan, G., Dong, G., Ye, L., and Qu, K.: Tennantite-(Ni), $Cu_6(Cu_4Ni_2)As_4S_{13}$, from Luobusa ophiolite, Tibet, China: a new Ni member of the tetrahedrite group, Mineral. Mag., 87, 591–598, 2023.

Warr, L. N.: IMA-CNMNC approved mineral symbols, Mineral. Mag., 85, 291–320, 2021.

Welch, M. D., Stanley, C. J., Spratt, J., and Mills, S. J.: Rozhdestvenskayaite $Ag_{10}Zn_2Sb_4S_{13}$ and argentotetrahedrite $Ag_6Cu_4(Fe^{2+},Zn)_2Sb_4S_{13}$: two Ag-dominant members of the tetrahedrite group, Eur. J. Mineral., 30, 1163–1172, 2018.

Wilson, A. J. C. (Ed.): International Tables for Crystallography Volume C: Mathematical, Physical and Chemical Tables, Kluwer Academic Publishers, Dordrecht, the Netherlands, 1992.

Wu, P., Yang, H., Qu, K., Wang, Y. J., and Gu, X. P.: Argentotetrahedrite-(Hg), $Ag_6(Cu_4Hg_2)Sb_4S_{13}$: a new tetrahedrite group mineral from the Dongping Hg-Ag deposit, Hunan Province, China, Acta Geol. Sin., 96, 418–425, 2022 (in Chinese with English abstract).